Chapter 6

Structure and Properties of the Bulk Standard Samples and Cellular Energy Absorbers

Pavel Kuznetcov, Anton Zhukov, Artem Deev,
Vitaliy Bobyr and Mikhail Staritcyn

Additional information is available at the end of the chapter

http://dx.doi.org/10.5772/intechopen.72973

Abstract

The development of additive technology revealed a real prospect of their use for the manufacture of complex shapes. Now, it is possible to produce parts that previously were either very difficult to produce using the subtracting technology and joining technology, or it was not at all feasible. In the manufacture of parts of complex shape, it is necessary to use a supporting structure, which is necessary to place such a way that they can be easily removed. Additionally, they must necessarily be absent in certain places. In this regard, the preparation model can take significant time to satisfy all of these, often conflicting, requirements. In this paper, we show optimization examples of the model preparation with support structures for parts manufactured at the facility EOSINT M270 and used in medicine and engineering. Additional emphasis is on the fact that, during the manufacture of parts, solidification's modes of massive parts differ from those of the thin-walled portions of parts. The results of the complex studies on the different stainless steels (including martensitic) are described with an emphasis on their structure and mechanical properties. The results of a honeycomb energy absorbers, which are quite seldom produced by the additive technologies, are presented in this chapter.

Keywords: additive technologies, selective laser melting, stainless steel, honeycomb structures, anisotropy, mechanical properties

1. Introduction

Since the late 1980s, generative manufacturing methods have been established as manufacturing systems for the product development in various sectors of industries. After only be used for the production of demonstration models (Rapid Prototyping, RP), the rapid tooling and

manufacturing now able to service a steady increasing range of applications. In order to achieve this status, the range of usable materials has been extended. Today, it is possible to process next to the RP area with omnipresent plastics, metallic standard materials, and ceramics. For the processing of metallic materials with the selective laser melting method, no binders or additives are necessary.

Additive manufacturing is a process in which an item is formed layer-by-layer, and taking into account the building principles, the presence of supporting structures is the necessary requirement for the complex shape and geometry items production, which are hard to obtain by classical (traditional) technologies [1, 2]. However, utilizing the supports, in some cases, it increases the time consumption and cost of the final product and it also has an effect on the finish surface treatment [3, 4]. Despite these disadvantages, the main advantage of the supports usage is the fact that it allows some heat output and therefore provides overall integrity especially of the complex elements [5]. Along with the selective laser melting process parameters, an item placement is very important, which itself provides a crucial input in the quality of the final product, as well as its correspondence to the given geometry and sizes [6].

The selective laser melting (SLM) is an additive manufacturing process. Complex components can be generated directly out of powdered metal on the base of CAD-Files. This manufacturing method is used for the manufacturing of tools for the plastic injection molding and the die casting. It is also possible to produce very filigree structures for dental and human implants. Today, diverse applications in the area of rapid prototyping, rapid tooling and rapid manufacturing are found. Currently, there are 10 materials qualified for this manufacturing method. These are high quality steels, titanium-, aluminum- and nickel-based alloys with powder grain sizes between 10 and 60 μm. The producible layer thickness is between 20 and 50 μm. It is possible to achieve a component accuracy of ±50 μm. The processing speed is 5–20 cm^3/h depending on the space utilization. The generated parts have a homogeneous structure and a density of almost 100%. Not only the physical but also the mechanical properties of the produced components comply with cast structures.

The manufacturing process of the SLM can be subdivided into three phases, which recur periodically. During the first phase, the substrate plate is lowered by one layer thickness. In the second phase, a new layer is applied on the substrate plate with the help of a coater. In the last step, the powder is scanned by the laser. Due to the absorbed energy, the powder fused at the scanned areas. This procedure will be repeated until the component is completed.

As a result of the layered build-up, the selective laser melting allows the manufacturing of components with hollows and undercuts. The developer gets a huge degree of freedom concerning the part geometry without being limited by restrictions of conventional manufacturing methods. In addition to that, it is possible to integrate multiple functions in the component. Thanks to this great freedom in design, it is also possible to individualize the products and to enlarge the number of variations arbitrary.

http://dx.doi.org/10.5772/intechopen.72973

In comparison to the indirect laser sintering processes, several process steps can be omitted like in infiltration of the part with other materials. Since the introduction of the SLM process, time-consuming and cost-intensive thermally after-treatments can also be substituted. The whole process chain and thereby the manufacturing time of the product can be reduced thanks to this change. In branches with very short product life cycles, the generated saving of time is a big competitive advantage. Especially in areas in which small lots of little components are required, the SLM process already became a competitive alternative to the conventional manufacturing methods. The metallic substructure of dental crowns can be manufactured with the help of the SLM process within 48 hours. In the SLM, the complexity of a component has only a low effect on the unit costs, because the costs of this process are more volume- than geometrical-based. The parts with a high degree of complexity are particularly suitable for the SLM, because its manufacturing with conventional processes is either very cost intensive or not possible.

Currently, SLM is used to manufacture functional prototypes and to build up final parts directly. In this case, the field of commercial applications is limited to single parts or parts in small batches. The tool- and mold-making industry is a typical example of a branch producing final parts in small batches of approximately one to eight. Because of the almost infinite geometrical freedom, SLM is applied to manufacture tooling inserts containing conformal cooling channels. Thanks to SLM, an improved tool cooling can be attained, resulting in reduced cycle times and improved part quality. As a result, the rapid manufacturing method SLM offers massive cost savings in combination with better functionalities despite the higher manufacturing costs for small batch production. Medical technology is another area applying the infinite geometrical freedom and variability of SLM. According to the current state of the art, individual implants in a batch size of one are manufactured with SLM. Typical examples of application are hip implants or surgical instruments out of titanium alloys as well as dental restorations out of cobalt chromium. Compared with conventional manufacturing methods like for example casting, SLM can significantly decrease the processing time and the production costs. Furthermore, the given geometric freedom can be used to manufacture implants with new functionalities such as hollow structures, graded porosity, adapted rigidity or surface structure.

Laser melting from metallic powders is a free form fabrication method causing great interest in the past decade. It has been reported recently that selective laser melting (SLM) using different alloys and steel powders is suited to create geometrically complex commercial components [7, 8]. Several reviews on SLM fabrication of 316L stainless steel were published [9, 10]. The influences of power, scanning speed, hutching, building direction on the microstructure and mechanical properties of fabricated 316L specimens have been studied; many researchers report on the effect of the material characteristics such as chemical composition, particle shape, size, and its distribution on laser melting of 316L stainless steel powder [10–12]. At present time, it is evident that SLM is a parameter sensitive process, and therefore for better understanding of these technology possibilities, it is necessary to get more information about mechanical and structural properties of standard specimens.

In the last years, additive technologies achieved a rapid boost, due to the requirements of the modern industry, including the increased productivity, achieving better properties and also lowering the technical and economic costs[13, 14]. Additive technology methods, specifically the SLM,

are widely used for the complex shape items and structures functional elements production [15]. Along the wide diversity of the metal powder materials, based on the stainless steels, which are commonly used in the SLM process, the martensite grade steels should be identified separately, because they are characterized by the non-equilibrium martensite structure and the inner stresses presence. A special interest is evoked, in case the SLM method utilization, by the 410L stainless steel, which represented by the quite simple chemical composition, that allows avoiding high segregation heterogeneity, although, the presence of a double α-γ transformation, requires special approaches for the 410L-based items production. Therefore, one of the main scientific objective, which is need to be solved, regarding the usage of martensite grade steels is an appraisal effect of the main technological parameters of the SLM process on the structure and mechanical properties of the producing items, because an overall integrity can only be achieved by utilizing an optimal methods and process parameters [16]. In addition, there is a necessity to implement an additional heat treatment, because of inner stresses and overall structure heterogeneity of the samples at the origin state after the laser melting process. In this connection, it seems important to try to find out whether it is possible to change the dispersion of the powder, the thickness of the melted layer, as well as the heat-input modes of its fusion to achieve a lower anisotropy.

Manufacturing of the cellular or thin-walled structures by the SLM is of a great scientific and practical interest [19]. It belongs to the fact that this approach allows to produce structures practically of any configuration and thickness, that is unobtainable or hard to achieve by the traditional methods [5]. Due to the possibility to obtain high values of specific mechanical and deformational properties in cellular or thin-walled structures, this kind of material is perspective to use in different areas: medicine, transport, machinery, aviation industries, etc.

Thin-walled cellular energy absorbing materials are widely used in different industry areas for the efficient energy damping in cases when it is necessary to immediately stop high speed transport vehicle. Based on the cellular structure of the energy absorber material, it is possible to manage the stop distance and maximum load [20–22].

We will start with a complex overview of methodological principles of the proper item placement (Section 2) during the building process. It will determine the future structure and mechanical properties of the produced items. In Section 3, we will determine the optimal SLM parameters to obtain the necessary properties of the common stainless steels like 316L, 321 and 410L. Also, it will be shown that there is a necessity to implement a heat treatment for the martensitic steels, allowing to increase overall mechanical features. And a short, Section 4 will highlight the possibility of obtaining the complex-shaped items like hexagonal energy absorbers and discuss structure and absorbing properties, implementing a quite amount of scientific investigations.

2. Methodology of choosing the proper item placement during the SLM process

One of the most complex areas during the item production is the inner hollows, access to which for the mechanical treatment is impossible. In this case, it is obligatory to place the item in such a way that there will be a possibility for the future treatment if it is necessary.

At first, let us describe the variants of supports placement and building on the example of two items: curved tube and micromotor, traditionally used in medicine area.

For the first example, let us take a look on the tube sample production approaches. It is well known that the time consumption of item manufacturing increases in proportion to its height. Therefore, the first and most obvious solution will be a horizontal item placement (**Figure 1a**). However, while producing an item, it is necessary that the inner surface of the curved tube will provide minimum defects quantity, and in case in their presence, there should be a possibility for their access and removal. Taking it into account, other placement variants will also occur unsuitable (**Figure 1b**, **c**) because of the defects formation on the curved area of the item (indicated by the black colored marker).

Therefore, it is stated that the only one suitable placement variant, providing the compromise, is the one presented in **Figure 1d**.

It should be mentioned that during the item preparation (designing), it was constantly advised to place supports inside the horizontal part of the tube and also on the outer side of the inclined part of the tube. While they are removed or shortened, the program has given the error notification. An image of the ready-to-use item is presented in **Figure 2**.

Another common problem during the item production is the support minimization. Also, it is preferable that the supports are absent in the places where after the production cycle it is practically impossible to perform the mechanical treatment because of the possibility to damage the items surface. As the second example, let us take a look at the micromotor sample. During

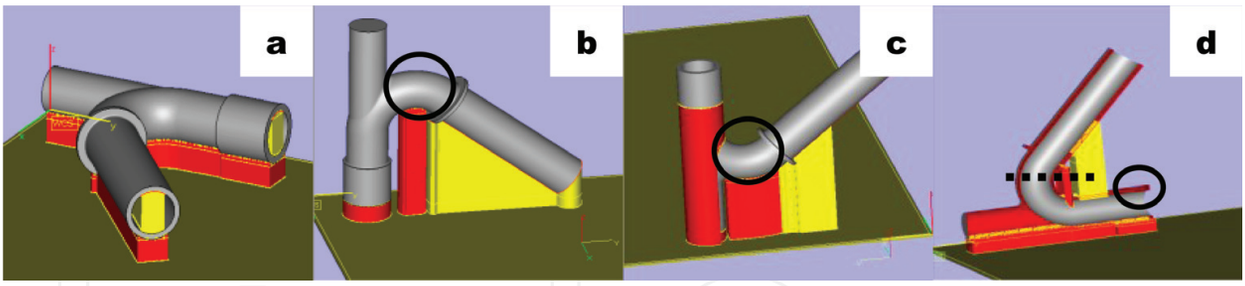

Figure 1. Examples of the supports disposal and "problem areas" indicating for the curved tube sample (a – supports inside the tube; b and c – circled areas, which are hard to complete using SLM; d – optimal item disposal).

Figure 2. An image of mechanically treated curved tube sample after the SLM process.

the production of such kind of items, it is necessary to provide the support absence on the micromotor blade surface.

Estimating the provided 3D model, it should me mentioned that the blades in their joints with the lower part have the limiting angle less than 45° (**Figure 3**), and at the same time, the necessary requirement is that the support is produced along the blade, until the angle will be 40° or more at its best, for better item production. Taking into account that the blades have enough thickness related to their height, therefore enough toughness, it is necessary to strengthen them and protect from the mechanical effect from the ceramic blade, performing the powder layer by designing the circuit support, beginning from the top part of the item and ending on the platform and the most important—that the circuit support should be adjoined with the blade edge (**Figure 3**). Under such requirements of the blade and the vertical support, an overall rigidity of the structure is increasing, providing the better chances for the item production (**Figure 3**).

Therefore, a proper item placement for the building process and supports placement optimization are the guarantee of a complex shape item qualitative production. At the present time, it is practically impossible to carry out such optimization using software options. The final decision is up to designer.

2.1. Structure features of the complex shape items produced by the SLM method

After the item building has finished, the first and major step is to investigate its quality and structure.

For the curved region, the micro sections were obtained in two planes: parallel and normally to the building plane of the sample. The structure images of the pipe sections are presented in **Figure 4**.

The structure analysis showed that in this case there are not many differences between the sample transverse and longitudinal cuts. All the pictures in **Figure 4** represent a quite uniform structure, despite the presence on a small amount of pores. In general, an important thing lies in the areas near the sample edges (especially the bottom part). In all the cases, the structure distortion is observed and the porous contamination is drastically increased. The maximum

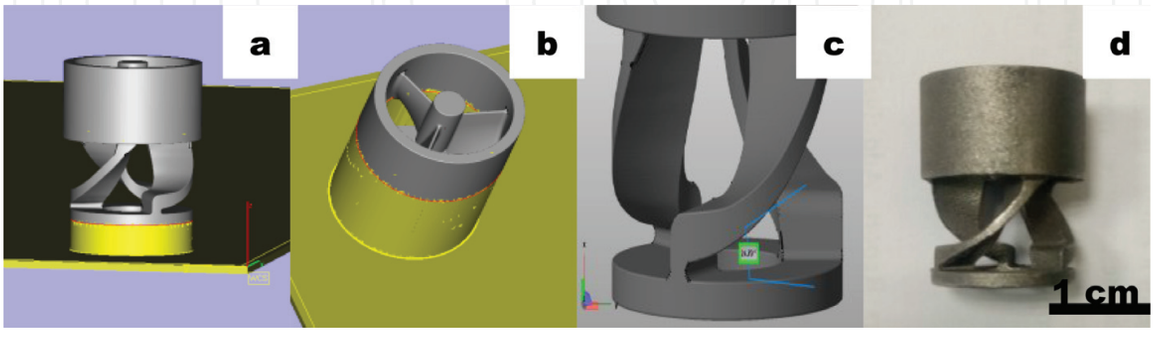

Figure 3. Different supports disposals and the limiting angle for the micromotor sample with the mechanically treated item (a – supports placement on the bottom part; b – optimal supports disposal; c –item after supports removal (the angle value on picture is 25°); d – mechanically treated item.

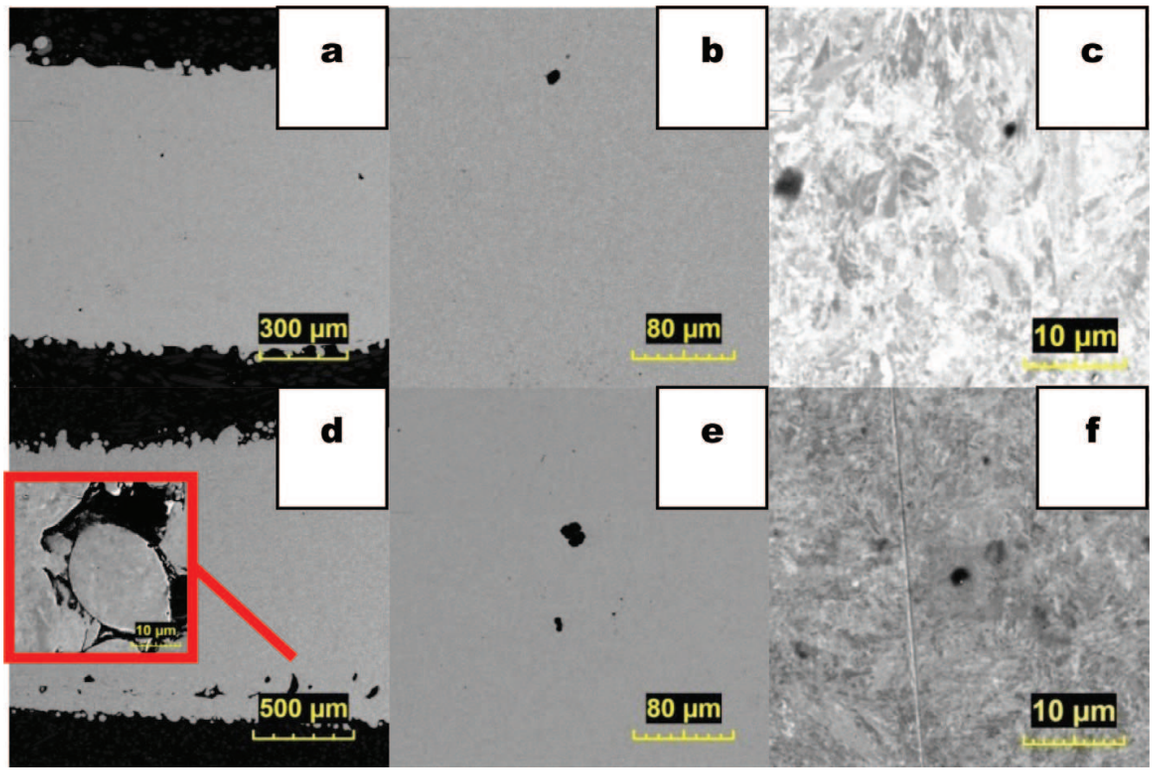

Figure 4. SEM structures obtained on the curved part of the tube: a, b, c—transverse cut; d, e, f—longitudinal cut (the scale in the red incut is 10 μm).

pore size is about 30–40 μm. It should be mentioned that the most part of the pores accumulates in the beside-contour layer.

As in **Figure 4**, the structure in its transverse direction practically does not differ from what we can see in **Figure 4a–c**. Separate crystallites are observed; an overall continuity is not violated; however, a small amount of pores is presented. Another pattern is observed on the longitudinal cut where porosity seems to be increased, and the pores in some cases consist from the unmelted components of the raw material (incut in **Figure 4d**).

Taking into account recommendations regarding the tube sample placement, according to the given variant in **Figure 1d**, the necessity occurred to perform investigations on the "problem area," marked with black circle. The main feature of this area is that during the selective laser melting process, the top part of the tube basis is closing up and there is a possibility to obtain some structure changes (**Figure 5**) because of the increased heat input.

The investigated area (around 1 cm width) is characterized by the irregular structure presence and a quite big amount of pores, up to 20 μm, which increases in case of longitudinal cut with some areas of "crumbly" structure, where along with the pores the unmelted particles of the raw powder materials are presented. During the SEM analysis, we also calculated the porous contamination in both cases. The lower amount we achieved is 0.8% on the transverse cut and the highest is 6.4% on longitudinal cut (**Figure 5b**, **d**; yellow color markers).

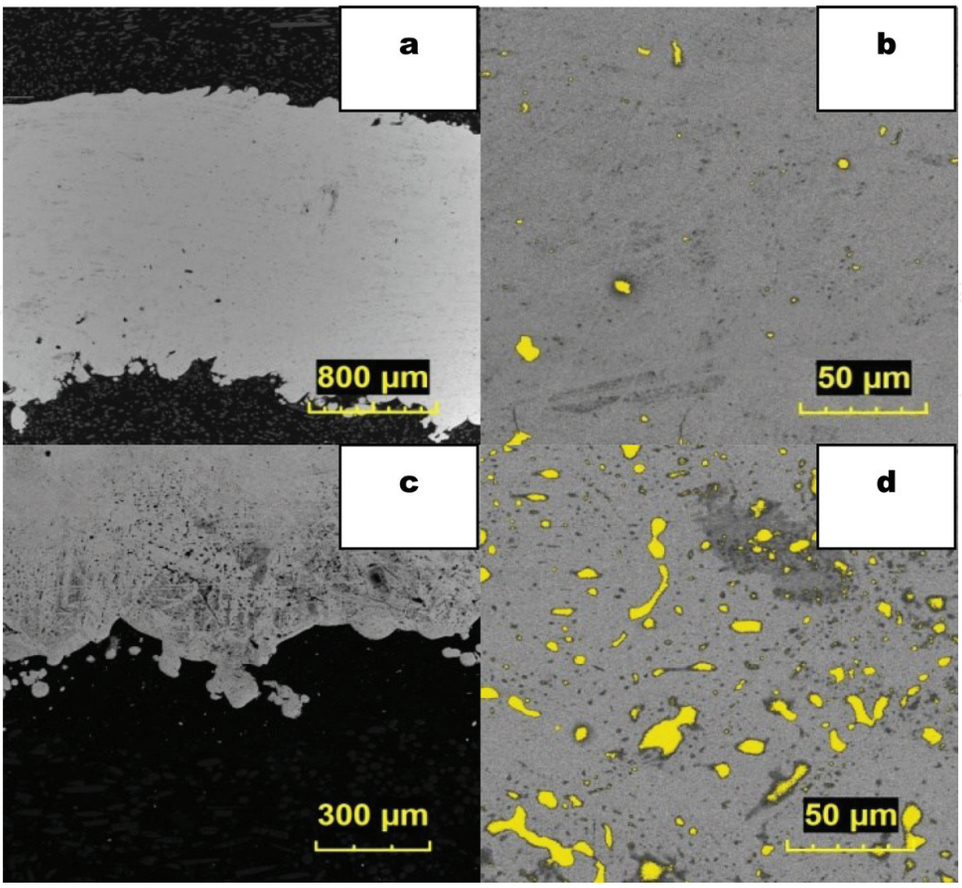

Figure 5. SEM structures obtained on the "problem area" of the tube: a, b—transverse cut; c, d—longitudinal cut.

As per the chosen items of curved tube and micromotor, an analysis of their proper placement and supports was carried out. It is stated that in case of the curved tube there is only one suitable disposal, since there will be no defects on the inner surface and the future mechanical treatment of these areas is drastically simplified. For the micromotor sample, we have found that there is a solution for building and elements under the 250 angle by the proper optimization of the supports placement. The porous content is changing in the range between 6.4 and 0.8%.

3. Structure and mechanical properties of austenitic and martensitic steel samples after SLM process

For estimating the mechanical properties, models for the uniaxial tension (ASTM E8) and impact strength (ASTM D6110) tests were designed and simultaneously to each other were manufactured on a single platform under nitrogen shielding atmosphere. Samples for the uniaxial tension had the working body diameter of 5–6 mm. Impact strength samples were produced with the square section of 10×10 mm^2. Horizontally built samples were already manufactured with the U-shaped notch in two ways (**Figure 6**). The notch on the vertically built samples was made during the finishing mechanical treatment. Three samples were made for each type of mechanical testing.

To investigate the building parameters effect, we have chosen three stainless steel-based powders: two austenitic (316L and 321) and one martensitic (410L). SEM images of the powder and their granular distribution are presented in **Figure 7**.

It is seen that for the 410L and 316L powders the distribution is thinner that for the 321 steel, which can affect on porosity and other properties during the items production. In **Figure 8**, the

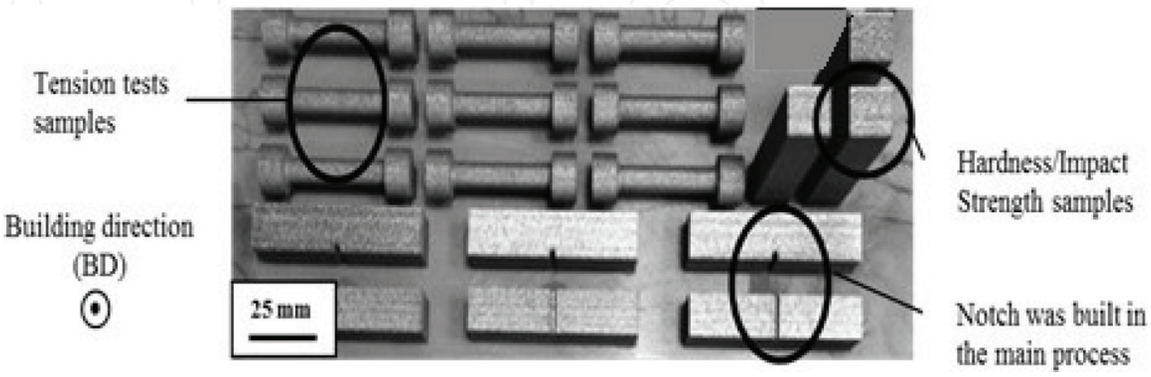

Figure 6. Platform fragment showing the samples placement.

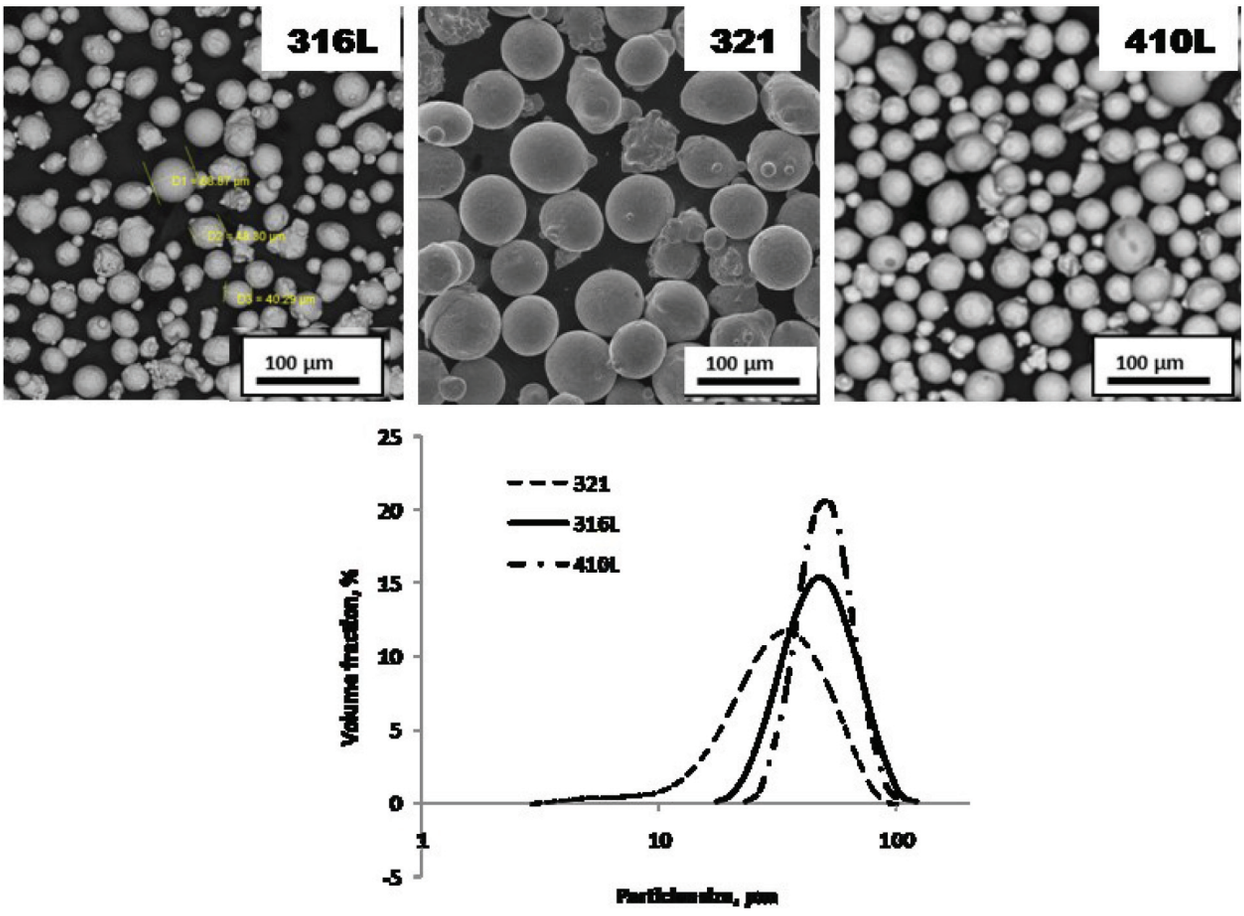

Figure 7. SEM images of the stainless steel powders and their granular distribution.

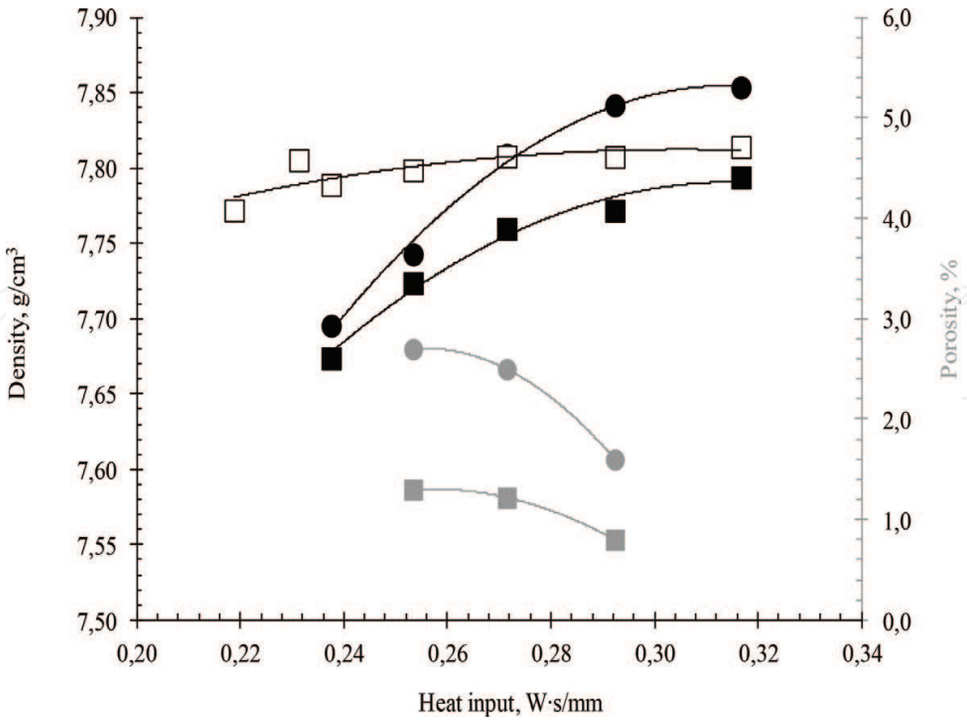

Figure 8. Dependences of the density (black lines) and porosity (gray lines) of steel samples vs. heat input; colored square symbols—Steel 321, layer thickness 40 μm; open square symbols—steel 321, layer thickness 20 μm; colored round symbols—316L steel, layer thickness 40 μm.

effect of layer thickness and level of energy input (calculated as a relation between laser beam power and scanning speed) for the 316L and 321 steels are presented.

The density and porosity of the samples are shown in **Figure 8**, from which it can be seen that the thickness of the melted layer significantly affects both characteristics. The smaller values of the density of samples, built at a 40-μm thick layer, can be explained by the presence of a larger number of pores and other inclusions. For samples from a larger 316L steel powder, the density increases more slowly with increasing heat input than in samples of a smaller 321 steel powder. It can also be concluded that the density values at 20 μm are closer to those for materials obtained by traditional metallurgical methods.

The results of the KCU tests for samples of 20 and 40 μm are shown in **Figure 9**, and a number of conclusions can be drawn from them. First of all, the KCU increases almost linearly with increasing energy input. In the range of values from 0.22 to 0.3 W s/mm, the anisotropy of KCU is maintained between horizontal and vertical samples. Secondly, samples from a larger powder of 316L steel obtained with a 40-μm thick layer, with increasing energy deposition, do not reach the same impact characteristics as the same obtained with a layer thickness of 20 μm. Samples of fine steel powder 321, formed with a layer thickness of 40 μm, possess the same impact properties as the samples formed with a 20 μm thick layer, with an increase in energy deposition by 1.5. Consequently, when using a larger powder, the growth of any parts with a layer thickness of more than 20 μm is not feasible.

It should also be noted that the KCU of the samples is 2–3 times lower than that of the samples from the same steels obtained by thermomechanical treatment. On the one hand, this may be

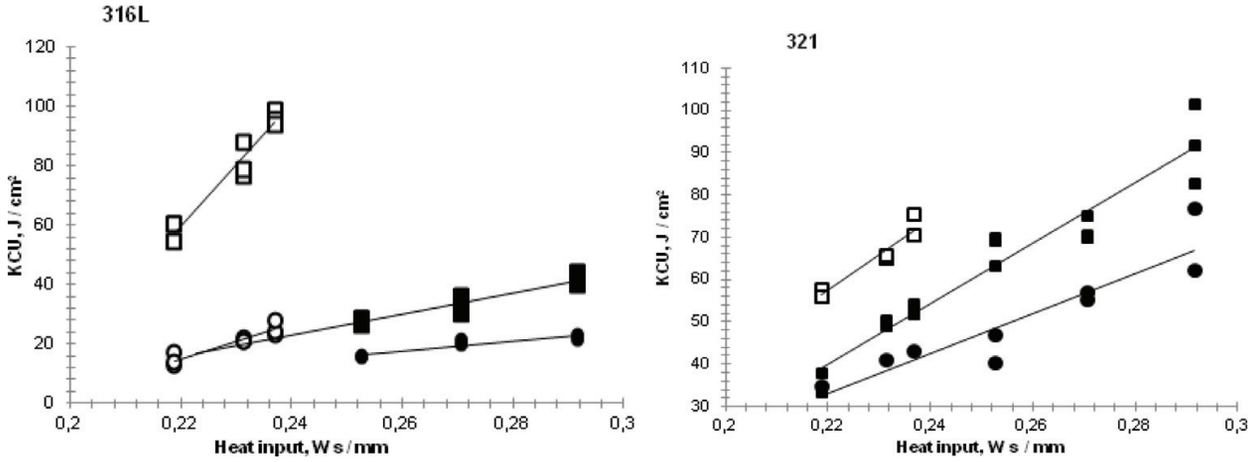

Figure 9. Dependences of the KCU of steel samples vs. heat input; square symbols—horizontal samples; round symbols—vertical samples, colored symbols—layer thickness 40 μm; open symbols—layer thickness 20 μm.

due to the fact that the notch of horizontal samples was applied in the model and formed during the building process. Taking into account the fact that in the building process the contour of the future layer is firstly melted by the laser, and then the layer itself is hatched, the microstructure of the contour layer will differ from the microstructure of the hatching layers. Thus, the KCU of a specimen with a mechanically made notch will be higher than that of a specimen with a grown notch [17]. However, even under such unequal conditions of testing, a rather large anisotropy is observed. On the other hand, this may be due to the presence of the pores in the samples of such dimensions that can affect the initiation of the crack during impact tests.

The results of mechanical tensile tests are shown in **Figure 10**. It can be seen that the anisotropy of mechanical properties is also preserved in all cases. To achieve the same mechanical properties at a thickness of the melted layer of 20 and 40 μm, it is necessary to increase the energy input by a factor of 1.5–2. It is noteworthy that the elongation of samples from steel 321 with increasing energy input to 0.27 and higher is no longer dependent on the building direction and comprise about 30–35%. This confirms that the presence of particles in the powder less than 20 μm positively affects the formation of mechanical properties.

A martensitic-based steel (410L) is standing beside the aforesaid ones due to the presence of a couple phase transformations, which can lead to some unacceptable results.

For the 410L steel, the hardness values measured on the sides of the standard samples showed that this property is independent from the samples disposal on the platform and it is linearly increasing with evaluation of the laser emitting power. The maximum hardness value was achieved at 190 W laser power and composed around 230 HB, which is more than the standard values for this type of steel around 195 HB. These hardness values (exceeding the standard ones) indicate the presence of residual stresses inside the structure.

It should be mentioned that the impact strength values of the as-build samples are practically independent of the U-shape notch disposal and laser power, composing meanly 5–6 J/cm^2. Herewith, after the heat treatment, these values are increasing linearly with the laser power growth from 17 to 32 J/cm^2, i.e. 3–6 times rise (**Figure 11**).

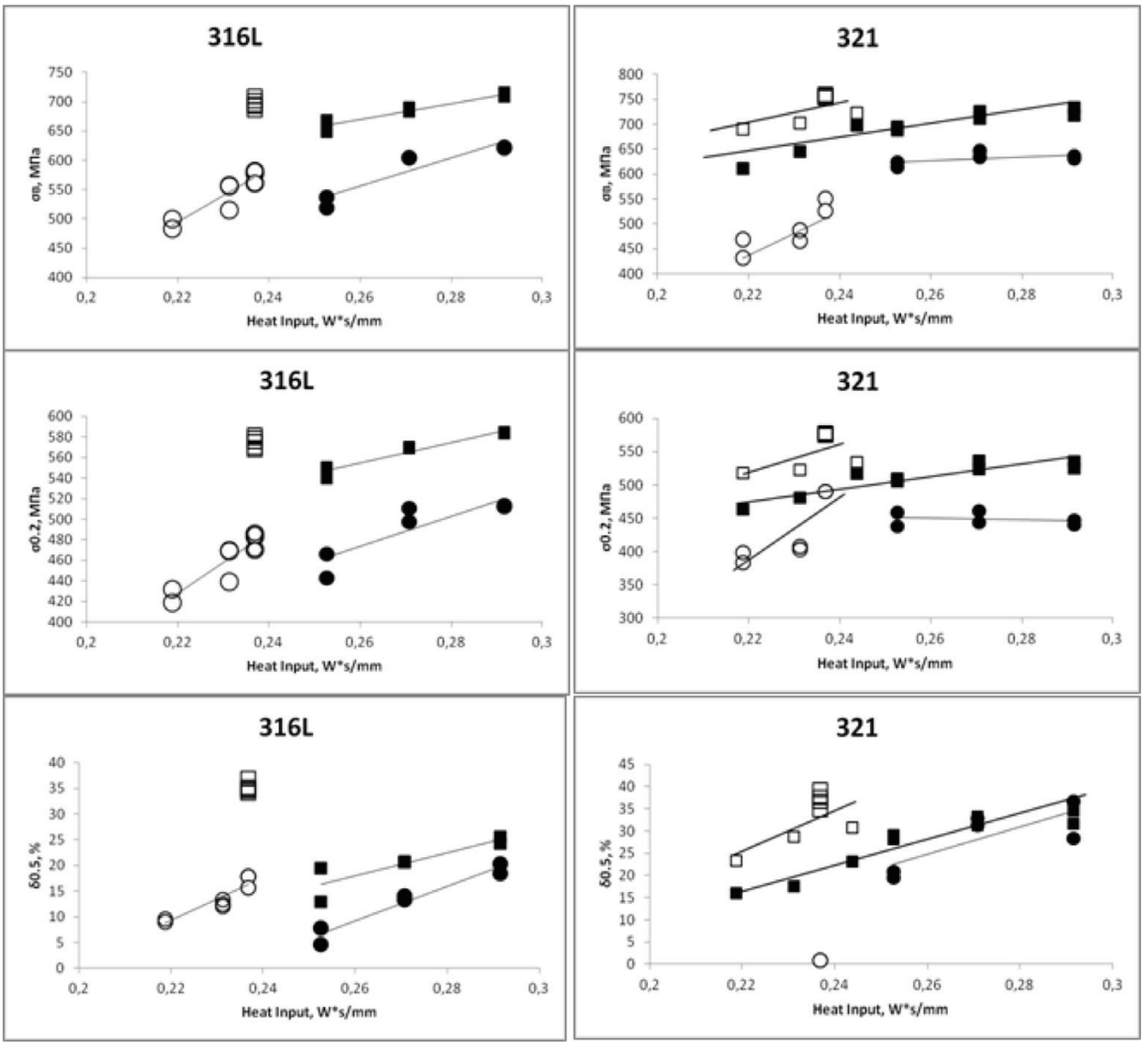

Figure 10. Dependences of the yield strength, tensile strength and elongation of samples from 316L and 321 steel from energy deposition made at a layer thickness of 20 and 40 μm; square symbols—horizontal samples; round symbols—vertical samples; open symbols—layer thickness 20 μm; colored symbols—40 μm.

The uniaxial tension tests of the as-build samples disposed horizontally and normally showed that in the last case, destruction is performed not by the samples body but in the attachment point. Drastically low values of relative elongation and diameter reduction are achieved, comprising 1.5 and 3.2%, respectively (**Figure 12c**). A completely different case was observed on the horizontally built samples, in which the tension occurred in the center of the sample body. It can be assumed that this is due to the structure as well as properties anisotropy of the additive material, depending on the samples disposal during the SLM process [17]. Presumably, such unsatisfactory values can be the result of the structural heterogeneity after SLM process.

For the horizontally built samples, the chart of the ultimate tensile strength (UTS), yield strength (YS) and relative elongation dependences from the laser emitting power is presented

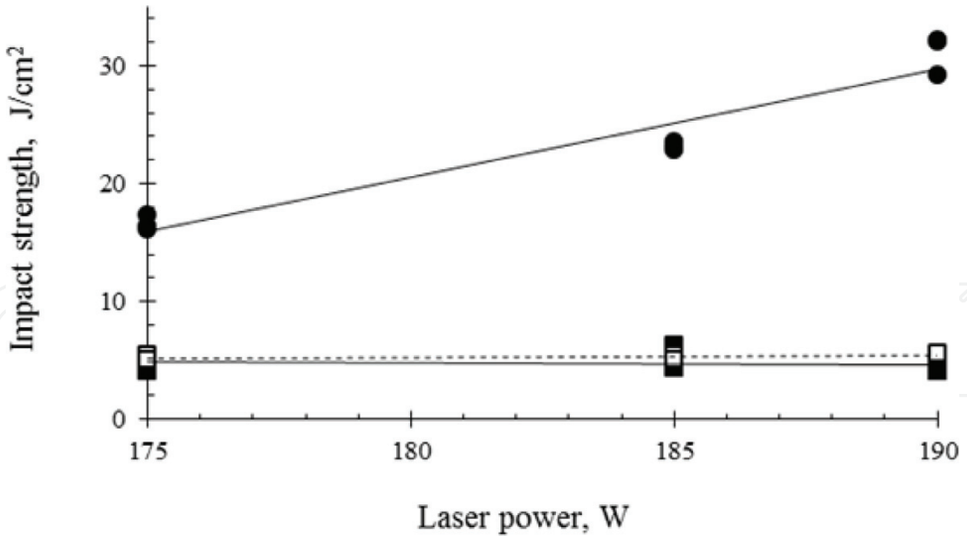

Figure 11. Impact strength dependency (prior and after heat treatment) from the laser power: square symbols—prior heat treatment (colored markers—notch in the building plane; open markers—notch normally to the building plane); round symbols—after heat treatment, notch in the building plane.

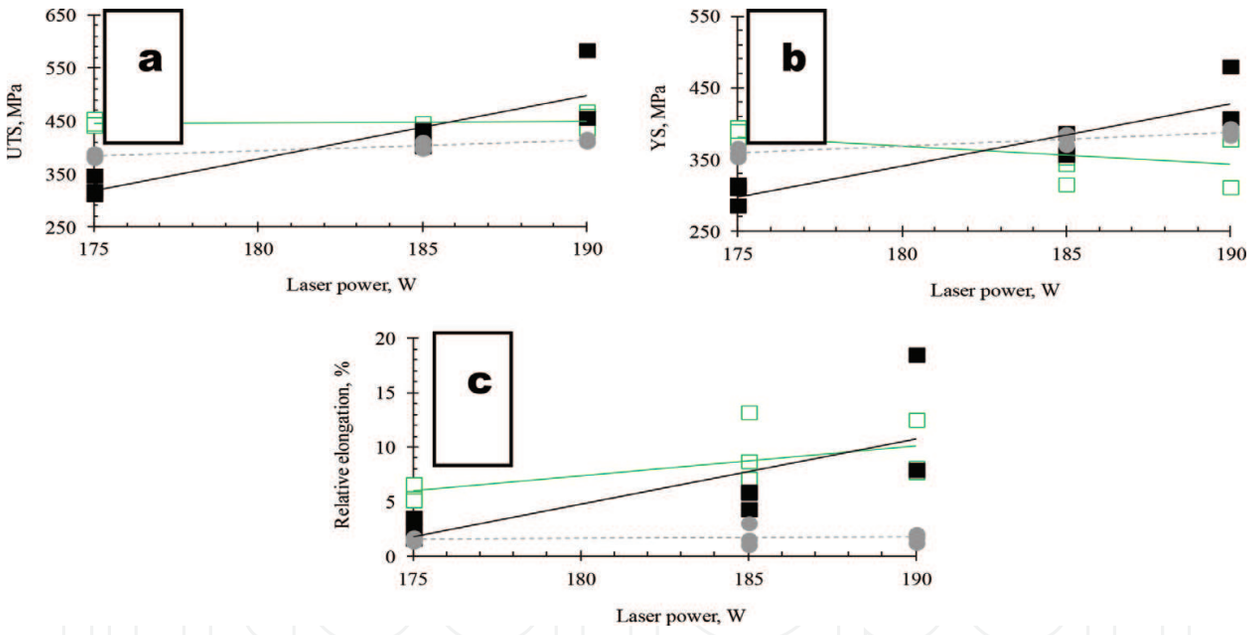

Figure 12. Strength properties dependency from the laser emitting power. Colored symbols—without heat treatment; opened—heat treated. Square symbols—horizontally built samples; round—vertically built samples (a – ultimate tensile strength dependency; b – yield strength dependency; c – relative elongation dependency).

in **Figure 12**. As it seen, the dependency is approximately linear and the values are increasing simultaneously with the laser emitting power.

The measured values of mechanical properties in the as-build state also correspond to the residual stresses, which drastically lower these numbers The possible way out of this problem is to implement a heat treatment. In this review, we have chosen to perform 2 cycle oil quenching-tempering treatment for trying to avoid the inner stresses content.

The carried out heat treatment (quenching and oil tempering), in general, allows increasing the UTS values, which are stay constant at the level of 450 MPa, independently from the laser emitting power (**Figure 12a**). The YS in contrary with the UTS is increased only at 175 W power. After further power growth, the investigated property value lowers, providing a linear tendency (**Figure 12b**). Also, a growth in the relative elongation values is observed in comparison with the nonheat-treated samples, which indicates on the deformational ability improvement of the material.

The similar increase of the KCU values occurred also after heat treatment (**Figure 11**). The maximum value is 30 J/cm^2 that corresponds to the requirements on this type of steels.

The performed mechanical tests and the achieved results showed that after the SLM process the structure state could be characterized by the inner stresses presence, which has an effect on properties, specifically on the impact strength. Providing the heat treatment allows removing the crystalline lattice distortions by the quenched martensite decay and lattice tetragonality rate lowering.

3.1. Samples structure

Structure investigation of the 316L and 410L steel was performed on the micro sections taken from the cross-cut of the specimens after testing.

Figure 13 shows layer-expressed austenitic structure, thickness and width of which are about 100 μm, which is 2.5 times more than the thickness of the powder layer and initial particle size. Also "big" grain's creeping is seen over the layer boundary, where non-metal (silicon and its oxides) inclusions are presented. One can say that the heredity of the orientations comes from layer to layer during the crystallization on the boundary.

A sample, obtained by the SLM process is characterized by the quasi-regular lamellar structure, that is specified by the fluctuations of chemical composition in the melt and crystallization areas. On the micro-sections in the EBSD analysis, an cambered with 20 ± 10 μm period crystallization fronts are observed, caused by the temperature pulsations and concentration heterogeneities (**Figure 14a**).

During the crystalline orientations, the transition zone, consisting of epitaxial layer and primary crystals, is not observed (**Figure 14a**). The orientation lines indicate only the contours of

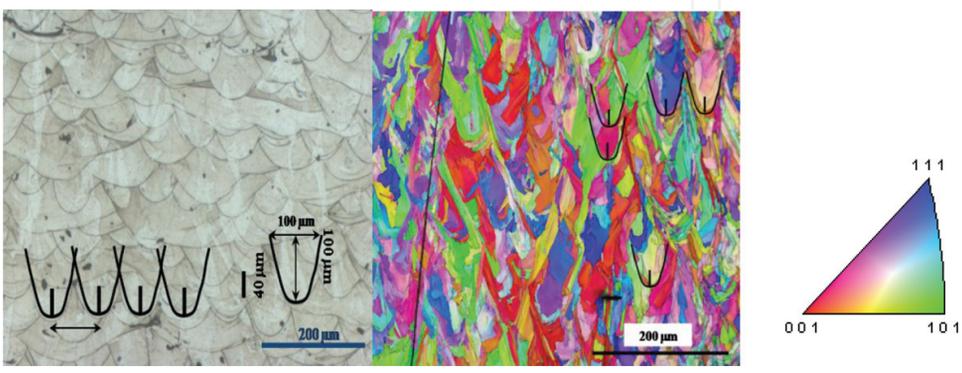

Figure 13. SEM and EBSD structures of the 316L-based sample after the SLM process.

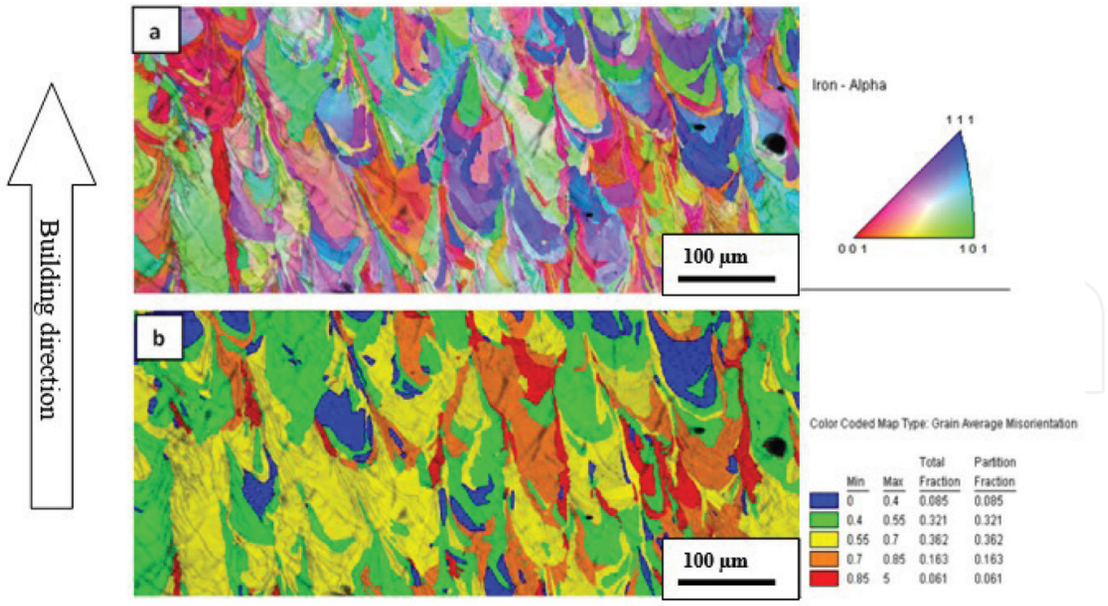

Figure 14. EBSD structures of the 410L-based sample after the SLM process (a – crystalline misorientations map; b – residual deformations map).

the powder melting zones. Because of the epitaxial growth of the crystals, formed during the solidification from the melt zone, it is occurred that the size of the primal crystals is moving towards the size of the origin powder particles. The crystalline size along the building direction is multiple times overcoming the depth of the melted layer. The misorientation character of the 410L steel grain boundaries is similar to the disorientations for the martensite steels, produced by the traditional technologies. The mean Ferre diameter and elongation of a single crystal are 68.17 and 0.289 μm, respectively. The bigger crystalline chords are orientated predominantly by ±20° with respect to the samples building direction. Within the crystallites, the disorientations of marked crystallographic directions are not exceed 5°.

Figure 14b represents the map of the residual deformations of the 410L-based sample in its as-build state (after SLM process), which confirms the inner stresses presence (red colored areas—quenched martensite) [18]. It should be mentioned that the blue colored areas, where the hardening is practically absent (tempered martensite area), are not common for the martensite steels; therefore, the problem of their presence in the structure is still unsolved. Phase analysis by the EBSD method shows that steel saves its one-phase austenitic structure, as no ferrite (alpha-phase) contents were detected.

In general, the EBSD analysis of the samples, produced by the SLM method, showed the obtaining the structure that is uncommon compares to the traditional methods of production. The "distinctive" feature of the structure such as grain epitaxial growth and their creeping over the layer boundary determines the final properties and overall quality of the product.

The carried out complex investigation of varying mechanical properties in dependence with laser power and mutual disposition with respect to the BD occurred to be quite important in case of determining the properties anisotropy. This fact on its turn will determine further utilization of these technologies in case of designing and producing more complex details and components of different machinery.

4. Cellular energy absorbing structures, produced by the SLM method

Traditionally, the cellular energy absorbers are produced from the thin corrugated sheets, joined to each other by different methods of gluing or welding [8, 20–22]. While using the additive technology, the main difference from the traditional one is that the cellular elements can be produced practically of any shape and the method itself is 100% waste-free, because no additional support structures are needed.

Samples with different wall thickness were modeled using CAD software. The 3D model of the honeycomb samples consists of 85 regular hexagons with the side length of 2.5 mm, stacked one to another and inscribed into the circle of 44 mm diameter (**Figure 15**). The height of the samples is 44 mm.

Prior the start of the compression tests, the structure of the samples was investigated. The common view of the hexagonal element with the wall structure of the samples from the side of electro-erosion cut and the EBSD structure analysis are presented in **Figures 16** and **17**, respectively. It is seen that the thin-walled element is produced quite well. The walls are connected under angle 118–1220. The wall thickness is uniform, and no deviations or "waviness" are observed. With the higher magnification, it is assured that the heavy expressed pores are absent. Also on the wall surface, it is clearly observed that a big cluster of small powder particles (less than 10 μm) always join the wall during the scanning process of the powder surface by the laser beam. Notably, particles of size more than 20 μm are absent on the surface.

Analyzing the EBSD maps, provided in **Figure 17**, we can make an assumption that the crystalline structure features are in relation with the building conditions. On the right picture, the changing of the structural state from the item surface to the center of the honeycomb element is noticed. As an example, a fine-crystalline structure in the contact zone between the melted item and powder raw material can be explained by the smaller powder particles gluing to the surface during building process. With the increasing distance from the item boundary deeply to the honeycomb joint, the temperature gradient lowers; therefore, the amount of grains per area unit

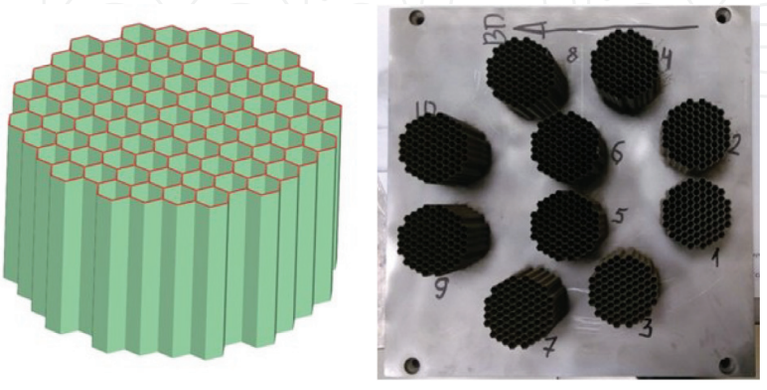

Figure 15. 3D-CAD model (on the left) and the produced samples on a single platform (on the right).

http://dx.doi.org/10.5772/intechopen.72973

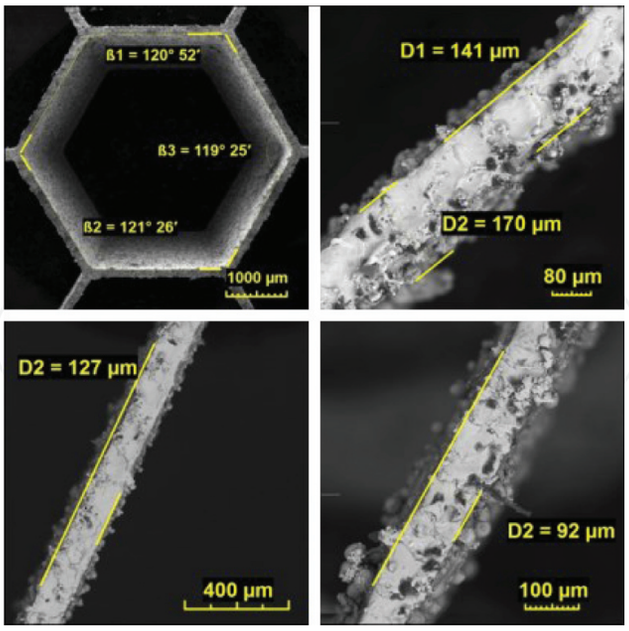

Figure 16. A typical view of the hexagonal element (on the left) and walls with different thickness (170, 127 and 92 µm).

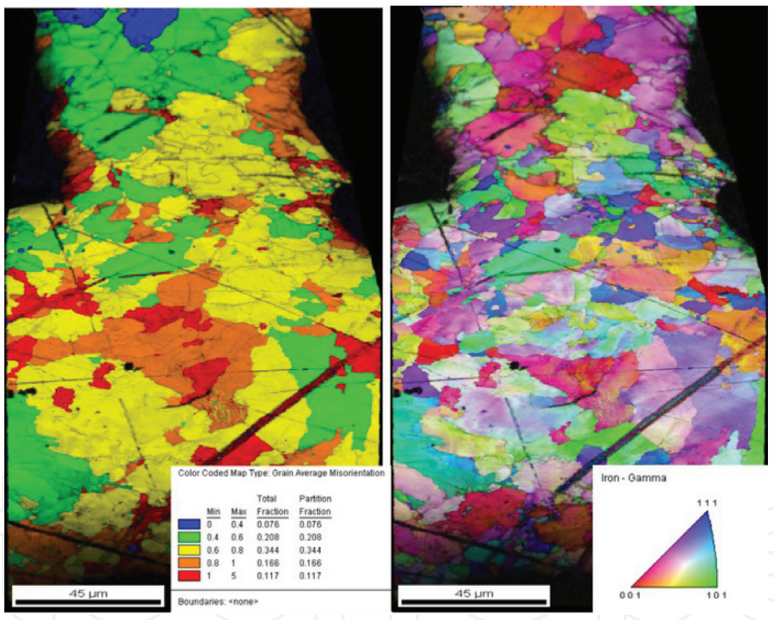

Figure 17. EBSD analysis of the central part of the honeycomb element.

also lowers. Moreover, in the results of EBSD maps analysis, we noticed an area in the centre of hexagonal structure joint (left picture) where the bending (misorientational) effect is prevailing. Such intergrain misorientation effect can be due to the elastic-plastic deformation and irregularity of the heat fields, affected by the laser beam scanning strategy during the melting.

An exterior of the samples after the compression tests and compression dependencies are presented in **Figure 18**.

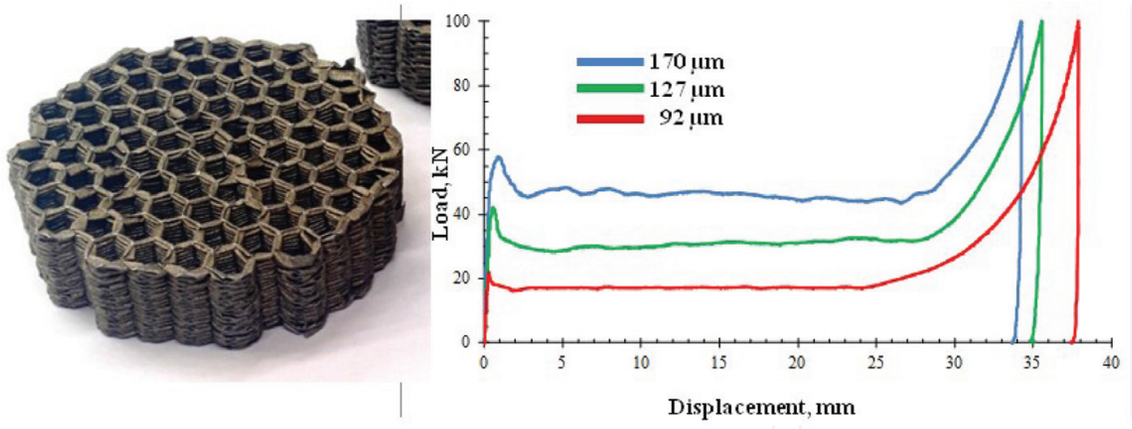

Figure 18. A typical view of the samples after compression tests (on the left) and load vs. displacement dependencies (on the right).

It can be seen that the samples were destructed uniformly without the size expansion. The reason can be the fact that during the samples compression process the uniform localized folding took place. The compression dependencies are looking familiar for these types of objects—a peak, corresponding to the activation load and a pace area, corresponding to the uniform destruction mode.

Crush force efficiency (CFE) is an important parameter to evaluate the performance of the structure during the crushing process, which is calculated as the ratio of activation load to compression load [23, 24]. Calculation CFE gives almost constant value from 0.7 to 0.8 that allows considering these structures as a good quality material produced by the selective laser melting [20–22].

Based on the example of the cellular structures, it was shown that utilization of additive technologies allows obtaining a material with high performance mechanical properties comparable to the traditional corrugation technologies. The minimum wall thickness is 92 μm.

5. Summary

This chapter has illustrated several complex challenges, facing which is common fact when utilizing additive technologies, more specifically—selective laser melting of metallic powders. It has been shown that there is only one suitable positioning of the item and its supports, which increases an overall quality and properties of the final product. Also, we have discussed a possibility to obtain samples from the different steel grades and pointed out the difficulties, occurred on the martensitic steel. Complex analysis of the mechanical testing results showed that the SLM-built samples provide increased mechanical properties compared to the traditionally manufactured (e.g. casting) ones. The structure obtained through the SLM process is uncommon to the standard structures of austenitic and martensitic grade steels. Production of the thin-walled honeycomb elements with the energy absorbing feature seems quite perspective, providing a waste-free technology with a results comparable to other manufacturing methods.

Acknowledgements

This work was supported by the grant of Russian Scientific Fund 15-19-00210.

Author details

Pavel Kuznetcov*, Anton Zhukov, Artem Deev, Vitaliy Bobyr and Mikhail Staritcyn

*Address all correspondence to: kspavel@mail.ru

National Research Center "Kurchatov Institute" – Central Research Institute of Structural Materials "Prometey", Saint-Petersburg, Russian Federation

References

[1] Vaidya R et al. Optimum support structure generation for additive manufacturing using unit cell structures and support removal constraint. Procedia Manufacturing. 2016;**5**:1043-1059

[2] Gardan N et al. Topological optimization of internal patterns and support in additive manufacturing. Journal of Manufacturing Systems. 2015;**37**(1):417-425

[3] Gan MX et al. Practical support structures for selective laser melting. Journal of Materials Processing Technology. 2016;**238**:474-484

[4] Jarvinen J-P et al. Characterization effect of support structures in laser additive manufacturing of stainless steel. Physics Procedia. 2014;**56**:72-81

[5] Das P et al. Optimum part build orientation in additive manufacturing for minimizing part errors and support structures. Procedia Manufacturing. 2015;**1**:343-354

[6] Manzhikov AV. Advances in theory of surface growth with applications to additive manufacturing technologies. Procedia Engineering. 2017;**173**:11-16

[7] Saeidi K et al. Hardened austenite steel with columnar sub-grain structure formed by laser melting. Materials Science & Engineering. 2015;**A625**:221-229

[8] Hanzl P et al. The influence of processing parameters on the mechanical properties of SLM parts. Procedia Engineering. 2015;**100**:1405-1413

[9] Gu D et al. Processing conditions and microstructural features of porous 316L stainless steel components by DMLS. Applied Surface Science. 2008;**255**:1880-1887

[10] Yandroitsev I et al. Hierarchical design principles of selective laser melting for high quality metallic objects. Additive Manufacturing. 2015;**7**:45-56

[11] Riemer A et al. On the fatigue crack growth behavior in 316L stainless steel manufactured by selective laser melting. Engineering Fracture Mechanics. 2014;**120**:15-25

[12] Zhong Y et al. Intragranular cellular segregation network structure strengthening 316L stainless steel prepared by selective laser melting. Journal of Nuclear Materials. 2016;**470**: 170-178

[13] Saedi K et al. Transformation of austenite to duplex austenite-ferrite assembly in annealed stainless steel 316L consolidated by laser melting. Journal of Alloys and Compounds. 2015; **633**:463-469

[14] Liu Y et al. Investigation into spatter behavior during selective laser melting of AISI 316L stainless steel powder. Materials and Design. 2015;**87**:797-806

[15] Sadlaka J et al. Study of materials produced by powder metallurgy using classical and modern additive laser technology. Procedia Engineering. 2015;**100**:1232-1241

[16] Krakhmalev P et al. In situ heat treatment in selective laser melted martensitic AISI 420 stainless steels. Materials and Design. 2010;**87**:380-385

[17] Deev A et al. Anisotropy of mechanical properties and its correlation with the structure of the stainless steel 316L produced by the SLM method. Physics Procedia. 2016;**83**:789-796

[18] Zisman A et al. Quantity attestation of bainite-martensite structures of the high strength alloyed steels by the scanning electron microscopy methods. Metallurgist. 2014;**11**:91-95

[19] Hadayati R et al. Mechanical properties of additively manufactured octagonal honeycombs. Materials Science and Engineering. 2016;**89**:1307-1317

[20] Partovi A. Numerical and experimental study of crashworthiness parameters of honeycomb structures. Thin-Walled Structures. 2014;**78**:87-94

[21] Pirmohammad S et al. Crushing behavior of new designed multi-cell members subjected to axial and oblique quasi-static loads. Thin-Walled Structures. 2016;**108**:291-304

[22] Xiea S. Crashworthiness analysis of multi-cell square tubes under axial loads. International Journal of Mechanical Sciences. 2017;**121**:106-118

[23] Wirzbicki T. Crushing analysis of metal honeycombs. International Journal of Inpact Engineering. 1983;**1**(Part 2):157-174

[24] Niendorf T. Lattice structures manufactured by SLM: On the effect of geometrical dimensions on microstructure evolution during processing. Metallurgical and Materials Transactions B. 2014;**45**:1181-1185